Met. Mater. Int., Vol. 23, No. 1 (2017), pp. 92~97
doi: 10.1007/s12540-017-6366-9

High Temperature Corrosion of Hot-Dip Aluminized Steel in Ar/1%SO_2 Gas

Muhammad Ali Abro[1,2] and Dong Bok Lee[1,*]

[1]School of Advanced Materials Science and Engineering, Sungkyunkwan University, Suwon 16419, Republic of Korea
[2]Department of Mechanical Engineering, Mehran University of Engineering and Technology, Jamshoro 76062, Pakistan

(received date: 25 May 2016 / accepted date: 24 July 2016)

Carbon steels were hot-dip aluminized in Al or Al-1at%Si baths, and corroded in Ar/1%SO_2 gas at 700-800 °C for up to 50 h. The aluminized layers consisted of not only an outer Al(Fe) topcoat that had inter-dispersed needle-like Al_3Fe particles but also an inner Al-Fe alloy layer that consisted of an outer Al_3Fe layer and an inner Al_5Fe_2 layer. The Si addition in the bath made the Al(Fe) topcoat thin and nonuniform, smoothened the tongue-like interface between the Al-Fe alloy layer and the substrate, and increased the microhardness of the aluminized layer. The aluminized steels exhibited good corrosion resistance by forming thin α-Al_2O_3 scales, along with a minor amount of iron oxides on the surface. The interdiffusion that occurred during heating made the aluminized layer thick and diffuse, resulting in the formation of Al_5Fe_2, AlFe and $AlFe_3$ layers. It also smoothened the tongue-like interface, and decreased the microhardness of the aluminized layer. The non-aluminized steel formed thick, nonadherent, nonprotective (Fe_3O_4, FeS)-mixed scales.

Keywords: metals, surface modification, oxidation, scanning electron microscopy (SEM), Al hot-dipping

1. INTRODUCTION

Hot-dip aluminizing is widely applied to the surface of steels to increase resistance to oxidation, corrosion and wear. It is an effective, low cost surface treatment technique, which forms coatings that protect the steel surface against high-temperature corrosive environments [1-5]. The aluminized coating consists of an Al topcoat and a multiple diffusive Al-containing underlayer. Industrially, aluminized steels are used for high-temperature applications, including mufflers, generators, boiler chimneys, burners, and pipes, all of which are exposed to corrosive steam or acids. The hot-dip aluminizing effectively improves the high-temperature corrosion resistance of steels by forming thin, dense Al_2O_3 surface scales [1,5-7]. Al-Si coated steels exhibit higher hardness than pure aluminized steel [8]. In this study, carbon steel was aluminized by hot dipping in molten Al or Al-1at%Si bath, and corroded in Ar/1%SO_2 gas at high temperatures. Sulfur dioxide dissociates through the reaction: $SO_2(g) \rightarrow 1/2S_2(g)+O_2(g)$. Sulfidation is considerably more harmful than oxidation, because sulfides are generally non-protective, friable, and grow rapidly. Hence, it is important to examine the corrosion behavior of the aluminized carbon steel in the SO_2 gas. Although the oxidation behavior of carbon steels hot dipped in Al [3,8,9,10] or Al-Si [1,3,5,7,8] molten baths has previously been reported, the corrosion behavior of carbon steels in SO_2 gas has not yet been adequately investigated.

2. EXPERIMENTAL PROCEDURES

The substrate was a medium carbon steel plate with a chemical composition of Fe-0.44C-0.30Mn-0.25Si-0.019S-0.016P in wt%. Hereafter, the compositions are denoted in atomic percentages (at%), unless otherwise stated. The substrate was ultrasonically cleaned in ethanol, immersed in 10 vol% HCl solution to remove surface oxides, treated with a liquid flux (20 vol% of KCl+AlF_3 in 4:1 wt. ratio solution in water), dried, and then dipped at 800 °C, on top of which a solid flux (KCl+NaCl+AlF_3 in 2:2:1 wt. ratio) was spread to protect the molten bath from oxidation. The dipping time was 5 and 20 min for the Al coating and Al-1%Si coating, respectively. The longer dipping time in the case of Al-1%Si coating was to obtain a thicker coating for detailed inspection of the coating. After aluminizing, the substrates were pulled out, air-cooled to room temperature, and further cleaned using 5 vol% HNO_3 solution to remove any flux remaining on the surface. The corrosion tests were performed by exposing

*Corresponding author: dlee@skku.ac.kr

the aluminized steel to the flowing Ar(99.999% purity)/1%SO_2(99.9% purity) gas at 700 and 800 °C for up to 50 h inside a tube furnace. The samples were analyzed by a high-power X-ray diffractometer (XRD) using Cu-Kα radiation operated at 40 kV and 100 mA, a scanning electron microscope (SEM) equipped with an energy dispersive spectroscope (EDS), and an electron probe microanalyzer (EPMA). The microhardness of the aluminized layer was measured along the coating depth with a Vickers microhardness tester under an indentation load of 200 g for 5 sec with a 50 μm indentation interval.

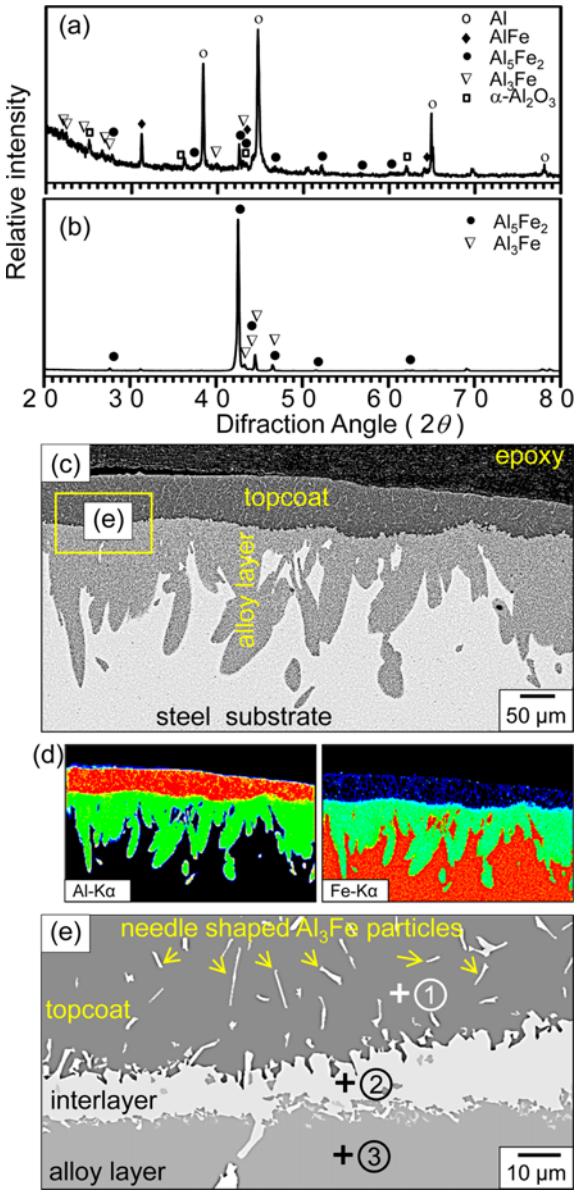

Fig. 1. Al hot dipped steel. (a) XRD pattern before grinding, (b) XRD pattern after grinding off the topcoat, (c) EPMA back-scattered electron (BSE) cross-sectional image, (d) EPMA maps of (c), (e) enlarged SEM image of rectangular area denoted in (c).

3. RESULTS AND DISCUSSION

Figure 1 shows XRD/EPMA/SEM results of the aluminized steel. In Fig. 1(a), Al peaks were stronger than other peaks of AlFe, Al_5Fe_2, Al_3Fe, and α-Al_2O_3. Peaks of Al came from the topcoat, and peaks of Al-Fe phases came from the underlayer or alloy layer. Peaks of α-Al_2O_3 came from α-Al_2O_3, which formed superficially on the aluminized coating through the reaction of Al with oxygen in air when the substrate was pulled out from the molten Al bath after hot dipping. After grinding off the Al-rich topcoat, the sample was X-rayed as shown in Fig. 1(b). This indicates that the alloy layer consisted primarily of Al_5Fe_2, together with a small amount of Al_3Fe. Fig. 1(c) shows the topcoat (thickness=45-75 μm), the Al-Fe alloy layer (thickness=25-250 μm), and the Fe-substrate. The topcoat was Al-rich, and had some dissolved Fe (Fig. 1(d)). Figure 1(d) shows the tongue-like morphology at the interface between the alloy layer and the substrate, which indicated that Al diffused unevenly from the Al melt into the Fe-substrate. The tongue-like morphology was formed for the following reasons. Firstly, Al_5Fe_2 has an orthorhombic structure with 30% of voids along the c-axis of the crystal structure so that it grows fast in a normal direction to the substrate (*viz*. along the diffusion direction) [2,11]. Secondly, the instability due to the difference in atomic size mismatch between Al (0.143 nm in radius) and Fe (0.126 nm in radius) leads to the non-uniform growth of the Al_5Fe_2 phase [11,12]. There was an interlayer (thickness=10-20 μm) between the topcoat and the alloy layer, as shown in Fig. 1(e). The EDS analysis indicated that the compositions of the spot ①, ②, and ③ were 98.63Al-1.07Fe-0.17Si-0.13Mn, 75.25Al-24.33Fe-0.25Si-0.17Mn, and 73.25Al-26.33Fe-0.25Si-0.17Mn (%), respectively. It is seen that the spot ①, ②, and ③ belonged to those of the Al-rich topcoat, Al_3Fe in the alloy layer, and Al_5Fe_2 in the alloy layer, respectively. The minor alloying elements such as Mn and Si dissolved throughout the aluminized coating. The composition of needle-like particles embedded in the Al-rich topcoat (Fig. 1(e)) matched with that of Al_3Fe [9,10,12].

Figure 2 shows EPMA/SEM results of the Al-1%Si hot-dipped steel. A topcoat with a thickness of 2-10 μm, an alloy layer with a thickness of 220-235 μm, and the substrate were shown in Fig. 2(a). The elemental distribution in the Al-rich topcoat and the Al-Fe alloy layer was displayed in Fig. 2(b). Silicon, which diffused inwardly together with Al from the melt, segregated mainly along grain boundaries of the alloy layer having the elongated columnar structure. Grain boundaries are an easy-diffusion path. Mn was deficient in the aluminized coating. The EDS analysis indicated that the compositions of the spot ①, ②, and ③ denoted in Fig. 2(c) were 98.4Al-0.92Fe-0.53Si-0.09Mn, 75.4Al-23.3Fe-1.23Si-0.1Mn, and 71.3Al-27Fe-1.5Si-0.2Mn (%), respectively. These compositions corresponded to those of the Al-rich topcoat, Al_3Fe in the

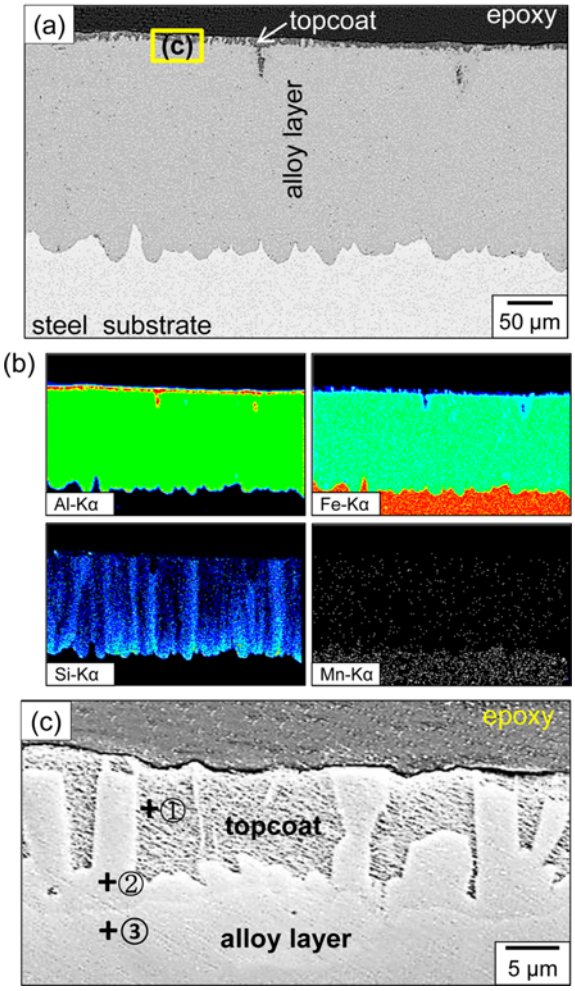

Fig. 2. Al-1%Si hot dipped steel. (a) EPMA BSE cross-sectional image, (b) EPMA maps of (a), (c) enlarged SEM image of the rectangular area denoted in (a).

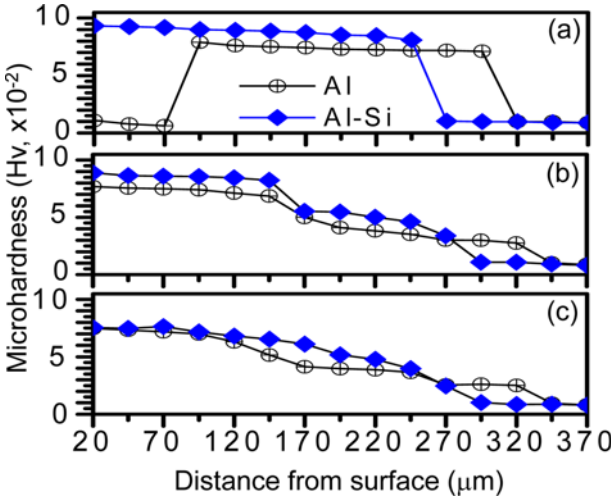

Fig. 3. Microhardness variation of Al and Al-1%Si hot-dipped steels along the coating depth. (a) after hot-dipping, and after heating in Ar/1%SO_2 gas for 50 h at (b) 700 °C, and (c) 800 °C.

alloy layer, and Al_5Fe_2 in the alloy layer, respectively. The Al-rich topcoat existed as discontinuous, grey polygons (Fig. 2(c)). The Si addition in the Al molten bath made the topcoat thinner, and nonuniform. It also smoothened the tongue-like interface by occupying vacancies in Al_5Fe_2, and thereby decreasing the diffusion rate of Al in Al_5Fe_2 [13,14] (Fig. 2(a)). The XRD analysis on the aluminized coating indicated that the alloy layer consisted primarily of Al_5Fe_2, including a small amount of Al_3Fe.

Figure 3 shows the variation of Vickers microhardness (Hv) along the coating depth before and after corrosion. For Al hot-dipped steel, the Al-Fe alloy layer (~738 Hv) was harder than the Al-rich topcoat (~83 Hv) and the steel substrate (~95 Hv) (Fig. 3(a)). For Al-1%Si hot-dipped steel, the Al-Fe alloy layer (~884 Hv) was harder than the steel substrate, and the Al-rich topcoat was not able to measure its hardness owing to its thinness (Fig. 3(a)). The Si addition increased the microhardness through the solid solution hardening [15]. The increase of the surface hardness makes the steel resistant to abrasion and wear [16], and broaden the operational range [6,8]. In Figs. 3(b) and (c), Hv values of the corroded samples were measured excluding the thin surface scale. Microhardness of the aluminized layer decreased with an increase in the heating temperature, because interdiffusion between the aluminized layer and the substrate made the aluminized layer diffuse and broad. Heating at 700-800 °C for 50 h transformed the Al-rich topcoat and Al_3Fe/Al_5Fe_2 intermetallics to Al_5Fe_2 and $AlFe/AlFe_3$ intermetallics. Similarly when oxidized in air at 750-950 °C, an AlFe layer formed between Al_5Fe_2 and steel substrate, pure Al-topcoat disappeared, and Al_5Fe_2 transformed to $AlFe/AlFe_3$ intermetallics to reduce the surface hardness [9].

The un-aluminized steel was entirely nonprotective in Ar/1%SO_2 gas, as shown in Fig. 4. The formed scale consisted of Fe_3O_4 as the major phase and FeS as the minor phase (Fig. 4(a)), indicating that the following reaction occurred: $5Fe+2SO_2 \rightarrow Fe_3O_4+2FeS$. In Fig. 4(b), the non-adherent scale was as thick as 1 mm, and continuously spalled off from the surface in the form of particles. The serious outward diffusion of cations to form the thick scale left behind Kirkendall voids in the scale. Voids can act as stress concentration sites to deteriorate the scale integrity or adherence, and provide easy diffusion paths [1,5,17]. The formation of a thick, (Fe_3O_4, FeS)-mixed scale (Fig. 4(c)) with voids generated large stress during scaling and the subsequent cooling stage, resulting in the partial detachment of the thick scale.

The Al hot dipping significantly improved the corrosion resistance of the steel, as can be seen from the comparison of Figs. 4 and 5. In Fig. 5(a), weak α-Al_2O_3 peaks and strong Al_5Fe_2 peaks were detected. Al in the topcoat reacted with impurity oxygen in Ar/1%SO_2 gas to become the extremely slowly growing α-Al_2O_3 scale, while unreacted Al in the topcoat

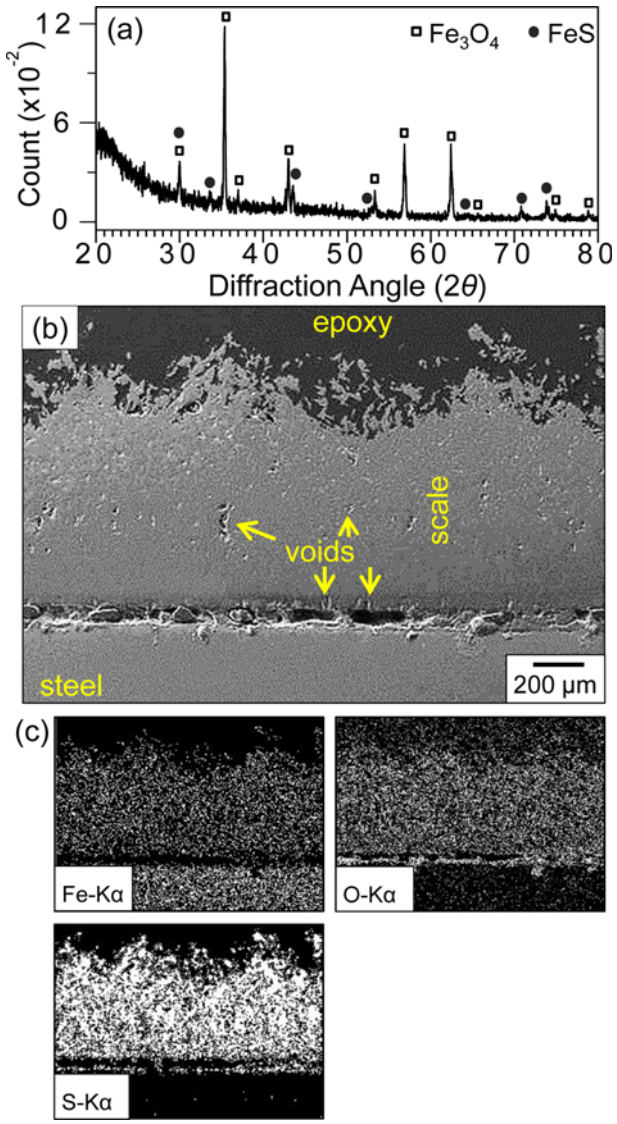

Fig. 4. Un-aluminized steel after corrosion at 700 °C for 50 h in Ar/1%SO_2 gas. (a) XRD pattern, (b) SEM cross-sectional image, (c) EDS maps of (b).

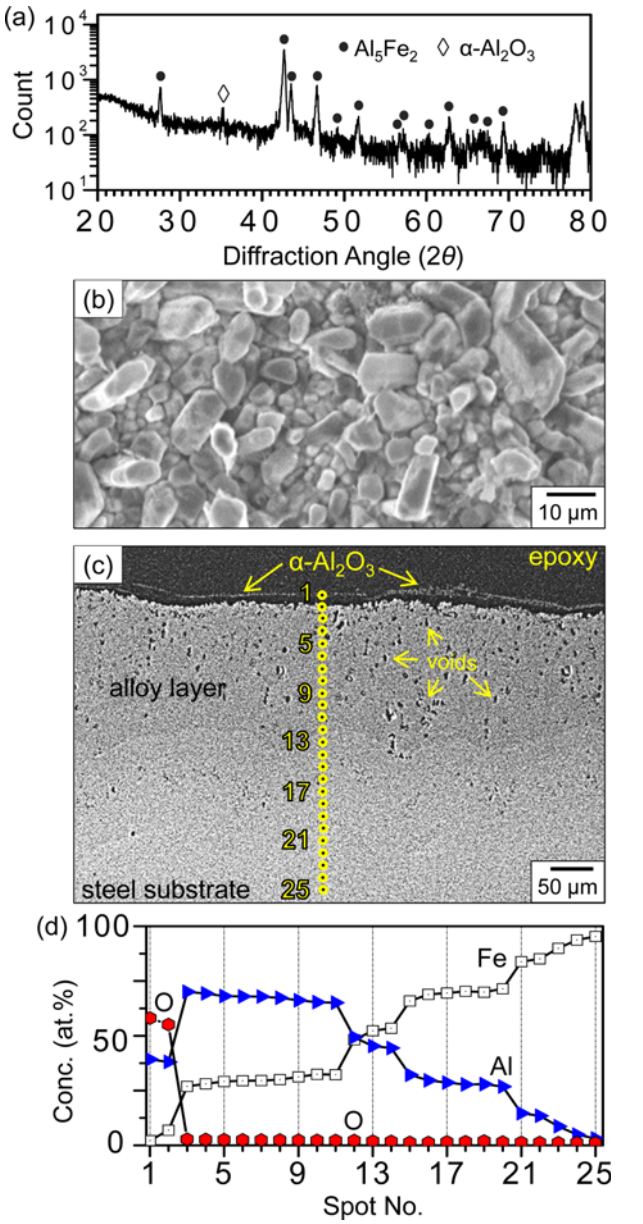

Fig. 5. Al hot dipped steel after corrosion at 700 °C for 50 h in Ar/1%SO_2 gas. (a) XRD pattern, (b) SEM top view, (c) SEM BSE cross-sectional image, (d) EDS concentration profiles along spots 1-25 denoted in (c).

transformed to the Al-Fe phase through interdiffusion. The scale was covered with round or elliptical α-Al_2O_3 grains (Fig. 5(b)). Figures 5(c) and (d) indicate that corrosion occurred only at the outermost surface because of the protective α-Al_2O_3 scale. Also, the tongue-like morphology shown in Fig. 1(c) changed to the wavy morphology owing to the interdiffusion between the aluminized layer and the steel substrate. The interdiffusion made the aluminized layer thicker and diffuse. The compositions of spot 1 and 2 were 58.1O-39.2Al-0.3S-0.2Si-2.2Fe and 55.1O-38.0Al-6.9Fe (%), respectively. Only at the spot 1, 0.3%S was detected, whereas Si originated from the substrate was intermittently detected inside the aluminized coating to a very small amount. The α-Al_2O_3 scale was intermixed with some iron oxides at the spot 1 and 2 (Fig. 5(d)). Not only the incorporation of sulfur at the spot 1 but also the difference of thermal expansion coefficients between the scale and the underlying

Table 1. Standard free energy change of the given reaction at 700 and 800 °C [18] and the Pilling-Bedworth ratio

Reaction	$\Delta G°$ (kJ/mol of S_2 or O_2)		P-B ratio (%)
	700 °C	800 °C	
2Fe(s)+S_2→ 2FeS(s)	-207	-186.8	261
2Fe(s)+O_2→ 2FeO(s)	-430	-404.8	168
4/3Al(s)+S_2→ 2/3Al_2S_3(s)	-448	-413.1	373
4/3Al(s)+O_2→ 2/3 α-Al_2O_3(s)	-935	-891.4	128

coating facilitated the spallation of the α-Al_2O_3 scale (Fig. 5(c)). The average compositions of spots 3-11, 12-15 and 16-20 corresponded roughly to Al_5Fe_2, AlFe and $AlFe_3$. The composition of the spot 25 was 1.1O-3.1Al-0.4Mn-95.4Fe (%), indicating that Al and oxygen diffused inwardly beyond the original aluminized layer during corrosion, according to the concentration gradient. It is noted that Al hot-dipped low carbon steel formed an Al_2O_3 scale, and $FeAl_2$/FeAl layers when exposed to air at 850 °C for 2 h, and an Al_2O_3 scale, and $FeAl_2$/FeAl/Fe_3Al layers when exposed to air at 950 °C for 2-8 h from the surface [10].

Table 1 lists the standard free energy changes for the oxidation and sulfidation at 700 and 800 °C [18], and the Pilling-Bedworth ratios of oxides and sulfides of Fe and Al. The most stable phase is α-Al_2O_3 so that α-Al_2O_3 was detected in Fig. 5(a).

The oxidation of Al and some Fe to the α-Al_2O_3-rich scale accompanied the volume expansion, resulting in the generation of compressive stress in the oxide scale and tensile stress in the aluminized layer [19]. This is another reason for the detachment of the scale shown in Fig. 5(c).

Figure 6 shows SEM/EPMA results of the Al hot dipped steel after corrosion at 800 °C for 50 h. The scale was again covered with round or elliptical grains, which consisted primarily

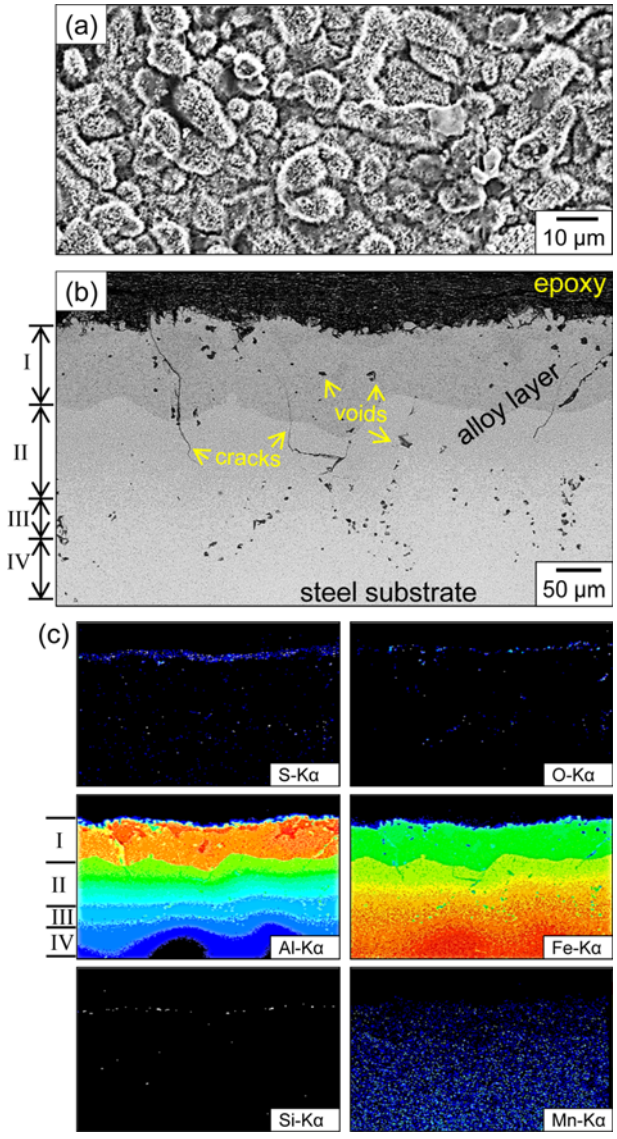

Fig. 6. Al hot dipped steel after corrosion at 800 °C for 50 h in Ar/1%SO_2 gas. (a) SEM top view, (b) EPMA BSE cross-sectional image, (c) EPMA maps of (b).

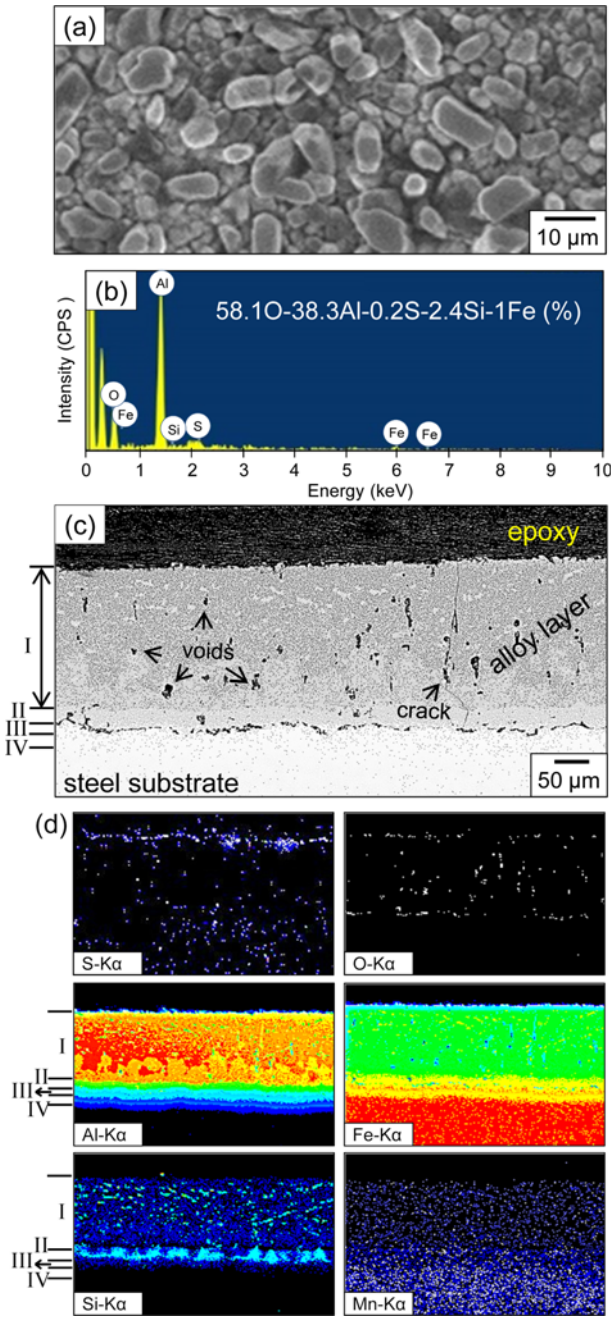

Fig. 7. Al-1%Si hot dipped steel after heating at 800 °C for 50 h in Ar/1%SO_2 gas. (a) SEM top view, (b) EDS spectrum of (a), (c) EPMA BSE cross-sectional image, (d) EPMA maps of (c).

of α-Al_2O_3 and some iron oxides (Fig. 6(a)). It was quite thin, because α-Al_2O_3 effectively suppressed the corrosion. It was however gone in Fig. 6(b) owing to not only its poor adherence resulting from the sulfur incorporation but also the thermal and growth stress developed in the scale. Heating made the coating broad and diffuse. A small amount of sulfur and oxygen was detected at the top surface (Fig. 6(c)). The average compositions of the layer I (70Al-27.4Fe-1.5O-1.1Si), II (48Al-49.5Fe-1.5O-1Mn), III (25.6Al-72Fe-1.2O-1.2Mn), and IV (14.8Al-82.1Fe-0.5O-1.2Mn) corresponded roughly to Al_5Fe_2, AlFe, $AlFe_3$, the Al-diffused α-Fe layer (i.e. α-Fe(Al)) and the substrate, respectively. The transformation of the Al-Fe intermetallics during heating generated cracks in the aluminized layer [8]. The outward diffusion of cations accompanied the formation of some Kirkendall voids. Cracks and the detachment of the scale would decrease the corrosion resistance especially during thermo-cyclings.

The Al-1%Si hot-dipping was also beneficial, as typically shown in Fig. 7. The high-temperature corrosion of Al-1%Si coated steel in Ar/1%SO_2 gas again led to the formation of round or elliptical grains at the surface (Fig. 7(a)). These grains consisted primarily of α-Al_2O_3, where Si, Fe and sulfur were incorporated (Fig. 7(b)). The surface scale shown in Fig. 7(a) was not visible in Fig. 7(c) due to its spallation. Kirkendall voids and cracks were observed in the coating, whose thickness was increased to about 300 μm owing to the interdiffusion during heating (Fig. 7(c)). In Figs. 7(c) and (d), the layer I (average composition; 68Al-24Fe-6.5O-0.5Mn-1Si), II (49Al-42Fe-7O-0.7Mn-1.3Si), III (25.6Al-65.3Fe-6O-0.5Mn-2.6Si), and IV (8.6Al-90.3Fe-0.2O-0.9Si) corresponded roughly to Al_5Fe_2, AlFe, $AlFe_3$, α-Fe(Al) and the substrate, respectively. Al, Si and oxygen diffused toward the substrate, according to the concentration gradient. Sulfur existed in the coating at the background noise level. The Si map shown in Fig. 7(d) indicates the pile-up of Si around the layer II and III. This resulted from the inward growth of Al-Fe alloy layer having a low Si solubility as well as the ensuing outward diffusion of iron from the layer II and III [20].

4. CONCLUSIONS

The aluminized layers that formed by hot dipping carbon steels in molten Al and Al-1at%Si bath consisted of an outer, thin Al topcoat, and an inner, thick Al-Fe alloy layer that consisted mainly of Al_5Fe_2, along with a small amount of Al_3Fe and AlFe. The Si addition increased the microhardness, and changed the interface between the substrate and the alloy layer from a tongue-like morphology to a wavy morphology. When corroded in Ar/1%SO_2 gas at 700-800 ℃ for up to 50 h, the aluminized steels exhibited good corrosion resistance by forming the thin α-Al_2O_3-rich scale, without forming nonprotective sulfides. Corrosion of the aluminized steels developed Al_5Fe_2/AlFe/$AlFe_3$/α-Fe(Al)) layers from the surface, decreased the microhardness, made the coating diffuse and broad through interdiffusion, and formed some Kirkendall voids and cracks in the coating.

ACKNOWLEDGEMENTS

This work was supported by the Korea Institute of Energy Technology Evaluation and Planning (KETEP) grant (No. 20143030050070) funded by the Korea government Ministry of Trade, Industry and Energy.

REFERENCES

1. C. J. Wang and S. M. Chen, *Surf. Coat. Tech.* **200**, 6601 (2006).
2. W. J. Cheng and C. J. Wang, *Appl. Surf. Sci.* **257**, 4663 (2011).
3. N. Ei-Mahallawy, M. Taha, M. Shady, A. Ei-Sissi, A. Attia, and W. Reif, *Mater. Sci. Tech.* **13**, 832 (1997).
4. M. S. Kwon and C. Y. Kang, *Korean J. Met. Mater.* **54**, 40 (2016).
5. I. I. Danzo, K. Verbeken, and Y. Houbaert, *Thin Solid Films* **520**, 1638 (2011).
6. M. A. Abro and D. B. Lee, *Metals* **6**, 38 (2016).
7. W. J. Cheng and C. J. Wang, *Mater. Charact.* **61**, 467 (2010).
8. T. V. Trung, S. K. Kim, M. J. Kim, S. K. Kim, S. J. Bong, and D. B. Lee, *Korean J. Met. Mater.* **50**, 575 (2012).
9. W. Deqing, *Appl. Surf. Sci.* **254**, 3026 (2008).
10. I. I. Danzo, Y. Houbaert, and K. Verbeken, *Surf. Coat. Tech*. **251**, 15 (2014).
11. W. J. Cheng and C. J. Wang, *Surf. Coat. Tech.* **204**, 824 (2009).
12. K. Bouche, F. Barbier, and A. Coulet, *Mat. Sci. Eng.* A **249**, 167 (1998).
13. M. V. Akdeniz, A. O. Mekhrabov, and T. Yilmaz, *Scripta Metall. Mater.* **31**, 1723 (1994).
14. G. Eggeler, W. Auer, and H. Kaesche, *J. Mater. Sci.* **21**, 3348 (1986).
15. R. A. Grange, C. R. Hribal, and L. F. Porter, *Metall. Trans. A* **8**, 1775 (1977).
16. K. Zaba, *Arch. Metall. Mater.* **56**, 871 (2011).
17. M. J. Kim and D. B. Lee, *Met. Mater. Int.* **22**, 430 (2016).
18. I. Barin, *Thermochemical Data of Pure Substances*, pp. 444-909, VCH, Germany (1989).
19. D. B Lee and M. J. Kim, *Korean. J. Met. Mater.* **53**, 406 (2015).
20. M. B. Lin and C. J. Wang, *Surf. Coat. Tech.* **205**, 1220 (2010).